

OPEN

## Effects of Composition of Alginate-Polyethylene Glycol Microcapsules and Transplant Site on Encapsulated Islet Graft Outcomes in Mice

Chiara Villa, PhD<sup>a,f,g<sup>+</sup></sup>; Vita Manzoli, MS<sup>a,h,<sup>+</sup></sup>; Maria M. Abreu, PhD<sup>a</sup>; Connor A. Verheyen<sup>b</sup>; Michael Seskin<sup>b</sup>; Mejdj Najjar, BS<sup>a</sup>; R. Damaris Molano, DVM<sup>a</sup>; Yvan Torrente, MD<sup>f,g</sup>; Camillo Ricordi, MD, PhD<sup>a,b,c,d,e</sup>; Alice A. Tomei, PhD<sup>a,b,c\*</sup>

<sup>a</sup>*Diabetes Research Institute, University of Miami Miller School of Medicine, Miami, FL, USA*

<sup>b</sup>*Department of Biomedical Engineering, University of Miami, Miami, FL, USA*

<sup>c</sup>*Department of Surgery, University of Miami Miller School of Medicine, Miami, Florida, USA*

<sup>d</sup>*Department of Microbiology and Immunology, University of Miami Miller School of Medicine, Miami, Florida, USA*

<sup>e</sup>*Department of Medicine, University of Miami Miller School of Medicine, Miami, Florida, USA*

<sup>f</sup>*Fondazione IRCCS Ca' Granda Ospedale Maggiore Policlinico, Milano, Italy*

<sup>g</sup>*Department of Pathophysiology and Transplantation, Università degli Studi di Milano, Italy*

<sup>h</sup>*Department of Electronics, Information and Bioengineering – Politecnico di Milano – Italy*

\*Corresponding author: Alice A. Tomei, 1450 NW 10<sup>th</sup> Avenue, Miami, FL-33136, USA; Phone: +1 305-243-3469; Email: atomei@miami.edu

<sup>+</sup>These authors contributed equally to the work

### **Author contributions**

A.A.T., R.D.M., Y.T., and C.R. designed research; C.V., V.M., M.N., M.M.A., C.V., M.S., and R.D.M. performed research; A.A.T., V.M., and C.V. analyzed data; A.A.T. directed the project, and A.A.T., C.V., V.M., and M.M.A. wrote the paper.

### **Disclosure**

A.A.T. is co-inventor of intellectual property used in the study and may gain royalties from future commercialization of the technology licensed to Converge Biotech Inc. C.R. is member of the scientific advisory board and stock option holders in Converge Biotech, licensee of some of the intellectual property used in this study. A.T. and R.D.M. are stock option holders in Converge Biotech.

### **Funding**

Funding was provided by philanthropic funds from the Diabetes Research Institute Foundation, grants from the Juvenile Diabetes Research Foundation (grant # 17-2001-268, 17-2010-5 and 17-2012-361), the Fondazione Tronchetti Provera, and the Fondazione IRCCS Ca' Granda Ospedale Maggiore Policlinico.

This is an open-access article distributed under the terms of the Creative Commons Attribution-Non Commercial-No Derivatives License 4.0 (CCBY-NC-ND), where it is permissible to download and share the work provided it is properly cited. The work cannot be changed in any way or used commercially.

ACCEPTED

## **Abbreviations**

**PEG**, polyethylene glycol

**ALG**, alginate

**Micro**, ALG microcapsules

**MicroMix**, hybrid ALG-PEG microcapsules

**Double**, ALG microcapsules covered with a 10-20 $\mu$ m-thick layer of PEG

**MRT**, median reversal time

**MST**, median survival time

**BG**, blood glucose

**DTT**, dithiothreitol

**GSIR**, glucose-stimulated insulin release

**OCR**, oxygen consumption rate

**T1D**, type-1 diabetes

## **Abstract**

### *Background*

Understanding the effects of capsule composition and transplantation site on graft outcomes of encapsulated islets will aid in the development of more effective strategies for islet transplantation without immunosuppression.

### *Methods*

Here we evaluated the effects of transplanting alginate (ALG)-based microcapsules (Micro) in the confined and well-vascularized epididymal fat pad (EFP) site, a model of the human omentum, as opposed to free-floating in the intraperitoneal cavity (IP) in mice. We also examined the effects of reinforcing ALG with polyethylene glycol (PEG). To allow transplantation in the EFP site, we minimized capsule size to  $500 \pm 17 \mu\text{m}$ . Unlike ALG, PEG resists osmotic stress, hence we generated hybrid microcapsules by mixing PEG and ALG (MicroMix) or by coating ALG capsules with a  $15 \pm 2 \mu\text{m}$  PEG layer (Double).

### *Results*

We found improved engraftment of fully allogeneic BALB/c islets in Micro capsules transplanted in the EFP (median reversal time MRT: 1d) vs. the IP site (MRT: 5d,  $p < 0.01$ ) in diabetic C57BL/6 mice and of Micro encapsulated (MRT: 8d) vs. naked (MRT: 36d,  $p < 0.01$ ) baboon islets transplanted in the EFP site. While In vitro viability and functionality of islets within MicroMix and Double capsules were comparable to Micro, addition of PEG to ALG in

MicroMix capsules improved engraftment of allogeneic islets in the IP site, but resulted deleterious in the EFP site, probably due to lower biocompatibility.

### *Conclusions*

Our results suggest that capsule composition and transplant site affect graft outcomes through their effects on nutrient availability, capsule stability, and biocompatibility.

ACCEPTED

## **Introduction**

Transplantation of pancreatic islets has shown great promise in achieving insulin independence and preventing type-1 diabetes (T1D) complications<sup>1</sup>. However, chronic immunosuppression is required to avoid rejection and recurrence of autoimmunity following transplantation. Chronic immunosuppression causes numerous adverse effects. Additionally, despite immunosuppression, 56% of the islet grafts lose function by 3 years after transplantation<sup>1</sup>.

Immunoisolation of pancreatic islets with biocompatible and permeable capsules may improve islet graft survival and allow for the reduction or total elimination of immunosuppression<sup>2-7</sup>. Despite 3 decades of research, effective clinical islet encapsulation has not been achieved for reasons yet to be completely understood. Key capsule parameters, including geometry, composition, and transplant site affect the outcome of encapsulated islet grafts and the optimal combination of such parameters might lead islet encapsulation to success. In this study, we focus on the specific effects of capsule transplant site and composition on graft outcomes while keeping a constant geometry (**Fig. 1A**). We used fixed-diameter spherical microcapsules that can be generated with traditional electrostatic droplet generator technology.

In order to evaluate the effects of the transplant site, we used alginate (ALG), a material that has been widely used for islet encapsulation<sup>8-18</sup>. Traditional ALG microcapsule diameters range from 600 to 1000 $\mu$ m with most of the volume being islet-free and biologically nonfunctional material<sup>19</sup>. Large amounts of bulk capsule material represent a barrier for transport of critical solutes to the islets, which could lead to core hypoxia and necrosis. Furthermore, large diffusion barriers hamper the transport of glucose and insulin through the capsule leading to a delay in glucose sensing and insulin secretion of the encapsulated islets<sup>20-22</sup>.

Finally, large capsule size may increase the volume of transplanted material up to 1000 times for capsule diameters of 1000 $\mu$ m in comparison to naked islets with the assumption that only 50% of capsules contain islets. Therefore, such volumes have so far limited the transplantation site to the intraperitoneal cavity (IP), which, unfortunately, is not an islet-friendly environment<sup>22-25</sup>. After transplantation in the IP site, capsules fall by gravity and aggregate in the lower abdomen worsening transport through the capsule. Here, we ask whether transplantation of minimized volumes of encapsulated islets in confined and vascularized sites, like the omental pouch in humans (a site we are currently testing in a phase I/II clinical trial with naked islets and chronic immunosuppression at the University of Miami Diabetes Research Institute) and the epididymal fat pad (EFP) in mice, can ameliorate the outcome of encapsulated allografts and of nonhuman primate (NHP) islet grafts in immunodeficient mice.

Unlike PEG, ALG is susceptible to swelling and rupture after transplantation due to osmotic stress leading to loss of immunoisolation and graft rejection<sup>26</sup>. Here, we ask whether transplantation of PEG-ALG hybrid 500 $\mu$ m-diameter micro capsules could ameliorate the outcome of encapsulated islet grafts in mice, especially in the IP site, where the graft is exposed to higher levels of osmotic pressure and mechanical stress than in the EFP site.

## **Materials & Methods**

**Encapsulation materials.** Micro capsules: ultra-pure medium viscosity sodium alginate (UP-MVG alginate, Novamatrix) at 1.2% w/v gelled with 50mM calcium chloride (CaCl<sub>2</sub>). MicroMix capsules: 1.2% UP-MVG - 5% w/v polyethylene glycol (PEG), functionalized (75%) with maleimide groups (PEG-MAL, 10kDa, 8-arms, Jenkem Technology custom synthesis) in 1ml of



1.2% UP-MVG solution. Double capsules: 5% w/v PEG-MAL crosslinked with Dithiothreitol (DTT, OmniPur, Calbiochem) in a 3:1 molar ratio of DTT to PEG.

**Islet isolation.** Animal studies were performed under protocol 13-042. Islets from Male BALB/c mice (Jackson Laboratories), Lewis rats (Envigo Laboratories, formerly Harlan) and non-human primate baboon (NHP; The Mannheimer Foundation, Inc., Homestead, FL, USA) were isolated as described elsewhere<sup>27,28</sup>.

**Osmotic pressure test.** Evaluation of mechanical stability of microcapsules was performed by osmotic pressure testing as previously described<sup>29</sup>.

**Fabrication of Double capsules.** 100µl UP-MVG Micro capsules were suspended in 1ml of 5% PEG-MAL (water phase). A solution of 50ml light mineral oil (Sigma Aldrich) and 5% Span80 (Sigma Aldrich) (oil phase) was formed by stirring at 350rpm for 2'. The water phase was added drop-by-drop to the center of the oil phase while the oil phase was continuously stirred at 350rpm. Five minutes after addition of the water phase to the oil phase, the DTT solution in DMSO was added to induce PEG-MAL gelation and the stirring speed was increased to 450rpm. PEG double coating was allowed to crosslink for 15 minutes and secondary beads were removed by filtration through a 250µm strainer (Thermo Scientific).

**In vitro assessment of viability and functionality of encapsulated islets.**

Static glucose-stimulated insulin release (GSIR) was utilized for assessment of islet function as previously described<sup>30</sup>. For viability assessment, naked and encapsulated islets were stained with calcein-AM (live cell marker) and ethidium bromide (dead cell marker) (live/dead viability kit, Molecular Probes), and imaged with a Leica SP5 inverted confocal microscope. Oxygen Consumption Rate (OCR) measurements were performed as previously described<sup>31</sup>.

**Engineered fibrin gels.** Fibrin gels were engineered for promoting rapid revascularization of embedded islets as previously described<sup>32</sup>.

**Diabetes Induction and Islet Transplantation in Mice.** Diabetes was induced in islet recipients by a single i.v. injection of streptozotocin (200 mg/kg; Sigma–Aldrich) as previously described<sup>30</sup>. For transplantation in the epididymal fat pad (EFP), 750 IEQ islets were distributed uniformly on the surface of the EFP and 20µl of engineered fibrin gels were then pipetted on the EFP to cover the islets. Graft function was monitored by measuring nonfasting blood glucose values. Reversal of diabetes was considered when mice maintained at least 3 consecutive blood glucose readings < 250mg/dL after islet transplantation. Graft rejection was considered when at least 3 consecutive blood glucose readings > 250mg/dL were detected in those mice that reversed diabetes following islet transplantation. For intraperitoneal (IP) islet transplantation, islets were injected into the peritoneal cavity in a total volume of approximately 0.2 ml. Transplantation in the renal subcapsular space (KD) was performed as previously described<sup>30</sup>.

*Additional information on Materials & Methods can be found in SDC, <http://links.lww.com/TP/B339>.*

## **Results**

### **Minimizing the volume of ALG microcapsules for transplantation in confined and vascularized sites**

We aimed at reducing the total volume of the encapsulated islet graft by (i) minimizing the diameter of the capsules while keeping a homogenous size distribution and (ii) maximizing islet-loading density while maintaining coating completeness. Keeping the ALG concentration

(1.2% w/v), the potential difference (8.8 kV) and the flow rate (10 $\mu$ l/min) constant, the average capsule diameter was decreased from 749 $\pm$ 35  $\mu$ m to 279 $\pm$ 29  $\mu$ m by reducing the needle internal diameter from 0.6 mm to 0.17 mm (**Table 1**). Pancreatic islets have a diameter of 50 to 350 $\mu$ m. Therefore, we chose 0.4 mm and not 0.17 mm as the internal diameter of the needle to encapsulate the islets. By reducing the flow rate of the alginate solution from 50 to 10  $\mu$ l/min while keeping the potential difference (8.8 kV) and the internal diameter of the needle (0.4 mm) constant, we were able to decrease the average capsule diameter from 651 $\pm$ 12  $\mu$ m to 526 $\pm$ 48  $\mu$ m (**Table 1, Fig. 1B**).

During the encapsulation process, we compared 3 different islet-loading densities: 500, 1500, and 3000 IEQ suspended in a volume of 100 $\mu$ l ALG (final islet density: 5k, 15k, and 30k IEQ/ml, respectively). We found that the 5k IEQ/ml density led to the highest percentage of cell-free capsules while the 30k IEQ/ml density results in multiple islets per capsule (**Fig. 1C**). Live / Dead staining and confocal imaging showed that capsules generated with 15k IEQ/ml islet density had higher cell viability than capsules with 30k IEQ/ml islet density (**Fig. 1D**). We also found that 15k IEQ/ml microencapsulated islets had similar GSIR function as to naked islets (**Fig. 1E-F**) in addition to homogeneous diameters (median 525 $\mu$ m, **Fig. 1G**).

We concluded that by using an electrostatic droplet generator, we could reduce the volume of standard alginate microcapsules to values that allowed transplantation in the EFP site in mice without impairing viability and function of encapsulated pancreatic islets.

## **Determining the effects of the transplantation site on engraftment and long-term function of ALG microcapsules in murine allografts and application to NHP islet grafts in immunodeficient mice**

In order to increase the pro-angiogenic potential of the EFP site we used a hydrogel that allows for extended release of pro-angiogenic factors and their synergistic signaling with extracellular matrix-binding domains in the posttransplant period <sup>32</sup>. We found that 750 IEQ naked islets reversed diabetes within 6 days (median reversal time, MRT: 1 day) after transplantation in the engineered EFP site while they did not reverse diabetes after transplantation in the IP site in fully MHC-mismatched chemically induced diabetic recipients (MRT: undefined  $p < 0.01$ ) (**Fig. 2A-B**). As expected naked islets promptly rejected within 27 days in the EFP site (median survival time, MST: 17 days). The same number of islets enclosed in ALG Micro capsules and implanted in the engineered EFP site reversed hyperglycemia as efficiently as naked islets (MRT: 1 day,  $p = 0.22$ ) (**Fig. 2A-B**) but, unlike naked islets, islets in Micro capsules were able to maintain euglycemia for more than 100 days (MST: undefined,  $p < 0.01$ ) in absence of immunosuppression (**Fig. 2A-C**). This confirms the effectiveness of ALG Micro capsules in preventing immune rejection. When implanted in the IP site, unlike naked islets, 750 IEQ encapsulated islets were able to reverse diabetes within 7 days (MRT: 5 days,  $p < 0.001$ ) but they did so with less efficiency than in the EFP site ( $p < 0.01$ ) (**Fig. 2A-B**). Finally, in the IP site, microencapsulated islets showed a trend towards decreased survival when compared to transplants in the EFP site (MST: undefined,  $p = 0.08$ ) (**Fig. 2C**).

Grafts retrieved 100 days after transplantation showed that the majority of the microcapsules analyzed ( $n = 5-7$ ) were intact. The islets within the capsules retrieved from the EFP site had no evidence of degranulation as determined by histological analysis (**Fig. 2D**) and

showed well-preserved architecture and strong insulin staining (**Fig. 2E-F**). This is indicative of long-term maintenance of islet viability. Conversely, islets within the capsules that were retrieved from the IP site showed central necrosis (**Fig. 2D**, arrows). Evident vascularization was observed in the peri-graft tissue in close proximity but not within the implanted capsules in the EFP site as assessed by CD31 immunofluorescence staining and confocal microscopy (**Fig. 2E**). Lack of CD3<sup>+</sup> T cells and B220<sup>+</sup> B cells capsule infiltration (**Fig. 2F**) indicates that incomplete survival of capsules in the IP site was not due to loss of immunoisolation.

We conclude that transplantation of islets in ALG microcapsules with minimized volume in a highly vascularized engineered EFP site improves engraftment and long-term function of allogeneic islets when compared to a free floating transplant configuration like the one in the IP site.

Next, we evaluated whether our novel transplantation approach could be translated to transplantation of a marginal mass of baboon NHP islets in immunodeficient and chemically diabetic NOD-*scid* mice. We found that baboon islets could be encapsulated in Micro capsules with the same protocol we optimized for rodent islets (**Fig. 2G**). More importantly, we found improved engraftment of 750 IEQ baboon islets in Micro capsules (MRT: 8d) vs. 1000 IEQ naked (MRT: 36d,  $p < 0.01$ ) islets transplanted in the EFP site. Grafts retrieved 30 days after transplantation showed that islets within Micro capsules had no evidence of degranulation as determined by histological analysis in comparison to naked islet grafts (**Fig. 2J**), which is indicative of maintenance of islet viability.

## **Design, Fabrication and in vitro evaluation of PEG-ALG hybrid MicroMix and Double capsules**

We found that unlike PEG, ALG capsules were not resistant to osmotic stress – ie capsule size increased within minutes of incubation either in saline or in H<sub>2</sub>O and dissolved within 60 minutes (**Fig. 3A-B**). More importantly, addition of PEG to ALG capsules improved the mechanical stability of ALG capsules (**Fig. 3A-B**).

Next, we fabricated **MicroMix** capsules (**Fig. 3C**) with the protocol previously optimized for ALG Micro capsules (**Fig. 1**) and Double coating of ALG Micro capsules with PEG (**Double**) by a new double emulsion method (described in the method section and **Fig. 3D**). We optimized the emulsion parameters to minimize the thickness of the PEG double coatings and the percentage of PEG-only secondary beads in order to maintain reduced graft volume and good biocompatibility<sup>33</sup>. Immunostaining with an anti-PEG antibody confirmed that PEG was uniformly distributed throughout the capsules in the MicroMix configuration while it was absent in the ALG capsules (negative control) and it formed a thin, uniform layer (15±2 µm thick) on 100% of the Double capsules (**Fig. 3E**). Spherical shape, average diameter, and size distribution of MicroMix and Double capsules were comparable to Micro capsules (**Fig. 3F-H**). Viability (**Fig. 3I**), GSIR (**Fig. 3J**, p>0.05) and oxygen consumption rate (OCR, **Fig. 3K**) of islets encapsulated in Micro, MicroMix and Double capsules were also comparable.

We concluded that reinforcement of ALG microcapsules with PEG improved capsule stability to osmotic stress without affecting capsule geometry or in vitro viability and function of encapsulated islets.

## Determining the effects of capsule composition on the outcome of PEG-ALG encapsulated islet allografts in mice

### *IP site*

When implanted in the IP site, islets within MicroMix capsules engrafted faster (MRT: 2 days) than islets within Micro capsules (MRT: 5 days,  $p < 0.05$ ) and naked islets (MRT: undefined,  $p < 0.01$ ) (**Fig. 4A-B**). Survival of islets within MicroMix capsules (MST: undefined) was comparable to islets within Micro capsules (MST: undefined,  $p = 0.77$ ) (**Fig. 4C**). Islets within Double capsules reversed diabetes only in 4/6 mice and showed some delay in reversal (MRT: 12 days), although not significantly different to islets within Micro ( $p = 0.15$ ) and MicroMix capsules ( $p = 0.07$ ). Survival of islets within Double capsules was comparable (MST: 94.5 days) to islets within Micro ( $p = 0.8$ ) and MicroMix ( $p = 0.62$ ) capsules (**Fig. 4C**).

Histological analysis of grafts that survived more than 100 days after transplantation revealed that the majority of Micro and MicroMix capsules did not present fibrotic outgrowths, capsule damage, and/or fracture (**Fig. 4D**). On the other hand, Double capsules were covered with a 2-layer-thick cell overgrowth and presented scattered pockets of inflammatory cells in a portion of the explanted capsules. Islets within Double capsules were fragmented and had a loss of pericapsular membrane, which is indicative of compromised viability and central necrosis (**Fig. 4D**). Immunofluorescence staining confirmed a higher proportion of insulin positive cells in islets enclosed in Micro and MicroMix capsules vs. Double capsules (**Fig. 4E-F**). Lack of macrophage (MAC2<sup>+</sup>, **Fig. 4E**), T and B cell (CD3<sup>+</sup> or B220<sup>+</sup>, respectively, **Fig. 4F**) deposition and penetration in all the capsule compositions suggested that capsules were immunoisolating.

We concluded that addition of PEG to ALG capsules in the MicroMix but not the Double configuration improved islet engraftment in the IP site while long-term islet survival was comparable.

### ***EFP site***

In the EFP site, islets within MicroMix capsules reversed diabetes slightly slower (MRT: 1.5 days) than islets in Micro capsules (MRT: 1 day,  $p < 0.05$ ) but comparable to naked islets ( $p = 0.75$ ) (**Fig. 5A-B**). Graft survival within MicroMix capsules (MST: 79 days) was inferior to Micro capsules (MST > 100 days,  $p < 0.05$ ) and not statistically different than naked islets (MST: 17 days,  $p = 0.19$ ) (**Fig. 5C**). Islets within Double capsules (MRT: undefined and only in 2/6 recipient mice) reversed diabetes less efficiently than naked islets ( $p < 0.01$ ), Micro ( $p < 0.01$ ), and MicroMix capsules ( $p < 0.05$ ) (**Fig. 5A-B**). Finally, islets within Double capsules (MST: 19 days) displayed poor survival in comparison to Micro capsules ( $p < 0.05$ ), but was not significantly different from MicroMix ( $p = 0.53$ ) or naked islets ( $p = 0.75$ ) (**Fig. 5C**).

Histological analysis of grafts surviving for more than 100 days after transplantation demonstrated that Micro and MicroMix capsules were intact and their spherical shape was preserved (**Fig. 5D**). Insulin staining of islets within Micro and MicroMix capsules revealed absence of either degranulation or central necrosis in Micro and MicroMix capsules indicating maintenance of overall viability (**Fig. 5E-F**). Host reaction at the capsule interface was slightly higher in MicroMix vs. Micro capsules as indicated by a 1 layer-thick cell overgrowth on the surface of MicroMix capsules (**Fig. 5D**). On the other hand, the host inflammatory response to Double capsules was markedly higher as shown by the thicker cellular overgrowth on the surface of those capsules (**Fig. 5D**). Islets within double capsules were fragmented and viability was



compromised (**Fig. 5E**). Lack of macrophages (MAC2<sup>+</sup>, Fig. 5E), T and B cells (CD3<sup>+</sup> or B220<sup>+</sup>, respectively, **Fig. 5F**) deposition or penetration in all the capsule compositions indicates that capsules were immunoisolating.

Next, we examined whether lower biocompatibility of MicroMix and Double capsules in comparison to that of Micro capsules was responsible for the reduced islet function. After implantation of empty capsules in the EFP, we found that Micro capsules displayed high biocompatibility with minimal cellular overgrowth and collagen deposition as assessed by trichrome staining (**Fig. 5G**). Inflammatory responses to MicroMix capsules (**Fig. 5H**) were stronger than Micro with slightly higher surface overgrowth. Double capsules, instead, displayed thick cellular overgrowth and fibrotic capsule formation on their surface (**Fig. 5I**).

Overall, we found that the addition of PEG as a reinforcement material to improve ALG stability (MicroMix) showed a benefit in improving islet engraftment when capsules were implanted in the free-floating configuration in the IP site but not in the EFP site. In the EFP confined and highly vascularized site, where the encapsulated islets were placed in direct contact with host tissue, the biocompatibility of the capsule material appeared to be slightly worse and likely affected graft outcome.

## **Discussion**

The success rate of microencapsulated islet allogeneic transplants in preclinical models is encouraging, but lack of translatability of preclinical results in effective clinical protocols is a current hurdle. Gaining a better understanding of the reasons for variability of preclinical results may help identify more effective strategies for better outcomes in future clinical trials.

The rationale for the work presented here was that capsule geometry, composition, and transplant site are the main determinants of the outcome of the encapsulated islet graft. Transport of nutrients to avascular islets relies on passive diffusion. Because diffusion rate depends on the diffusion distance, reducing the capsule diameter from 800 $\mu$ m to 500 $\mu$ m, as we successfully achieved, likely improved transport of nutrients including oxygen, to the islet core, positively impacting islet viability and GSIR function. Nutrient consumption rate inside the capsule is proportional to the number of cells. By comparing the effects of different islet loading densities we concluded that a 15k IEQ/ml (3%) loading density was a good compromise between minimizing graft volume and maximizing islet viability. This result represents an improvement over traditional loading densities (0.8-1.5%).

Reducing the capsule diameter from 800 $\mu$ m (64-fold increase in graft volume compared to naked islets) to 500 $\mu$ m (15.6-fold increase in graft volume compared to naked islets) was associated with a 4-fold reduction of the total volume of the encapsulated islet graft and allowed us to transplant encapsulated islets in the confined and highly vascularized EFP site. This allowed us to evaluate the importance of the transplant site in promoting engraftment and long-term survival of encapsulated islets. We have previously shown that presence of pro-angiogenic gels improves the outcome of naked islet grafts in the EFP site <sup>32</sup>. Here we evaluated the potential beneficial effects of transplanting encapsulated islets in a confined site with the highest pro-angiogenic potential (with inclusion of pro-angiogenic gels) vs. a site where encapsulated islets remain free-floating and cannot get revascularized (IP). Delays in oxygen transport to the islet core in the IP site might have caused the central necrosis phenomenon that we observed in encapsulated islets in the IP but not the EFP site. The fibrotic overgrowth of Double capsules due to poorer biocompatibility observed histologically might have caused a delay in glucose and

insulin diffusion through the peritoneal membrane and the capsule and caused loss of a portion of the islet graft. This in turn might be the reason for longer reversal time and the presence of more pronounced blood glucose fluctuations that were observed for Double capsules in the IP site. Lack of T and B cell recruitment and infiltration into the capsules in all conditions further confirmed that reduced long-term graft survival was not due to lack of immunoisolation and immune rejection of transplanted islets, but was likely dependent on islet death because of insufficient transport of nutrients.

Transplantation in the EFP site may not only enhance nutrient transport due to the proximity of host vessels to the encapsulated graft, but also may provide protection from mechanical stress at the implant site by confining the graft between 2 mesothelial layers and preventing shear stress due to graft displacement. Both enhanced nutrient transport and protection from mechanical stress are determining factors for long-term survival of encapsulated islets. We found that the more stable MicroMix capsules improved islet engraftment in the IP site where higher mechanical protection is needed but not in the EFP site where higher stability may not be critical for islet function, and where capsule biocompatibility may play a predominant role in determining the outcome of the encapsulated graft. Conversely, Double capsules did not show any improvement in islet engraftment and long-term function over ALG capsules in the IP site. In fact, they had worse outcomes in the EFP site. This is likely due to the fact that any beneficial effects of higher stability conferred by PEG double coatings may not outweigh the observed poor biocompatibility. This is in contrast with our previous studies on conformal coating encapsulation with PEG hydrogels where we did not observe such high fibrotic reaction to thin and conformal PEG coatings. Potentially, worse biocompatibility of Double coatings may come from the presence of secondary particles generated by the double emulsion technology.

Secondary particles are smaller and therefore less biocompatible than 500 $\mu$ m capsules<sup>33</sup>. Furthermore, worse biocompatibility of PEG Double coatings may be due to the larger surface area and total volume of PEG double coatings vs. conformal coatings, as well as the different transplant site (EFP and IP here vs. the kidney capsule in<sup>30</sup>).

While the improvement to achieve normoglycemia in mice transplanted in the EFP vs. the IP site was a matter of a few days, this could be due to the relatively high dose of islets transplanted in each mouse. While a few days might seem trivial in mice, the difference in diabetes reversal of a few days with full islet mass may translate into a dramatically bigger effect when suboptimal islet doses are transplanted in larger animals and humans. This is supported by our results from transplantation of a marginal mass of NHP islets in the EFP site of immunodeficient mice showing diabetes reversal and sustained function of baboon islets within Micro capsules optimized to minimize the graft volume. Further work is required to validate our approach and begin to understand the effects of islet encapsulation in autoimmune models of diabetes where additional challenges may require further modifications of our transplantation protocol.

Our results suggest that future clinical trials should be designed to determine whether transplantation of encapsulated islets in clinically relevant confined and vascularized sites, like the omentum, might increase the efficacy of encapsulated islet grafts in humans. We anticipate that application of our findings to improved capsule geometries where coating thickness is minimized will provide additional improvement to the outcome of encapsulated islet grafts and will benefit the field of islet transplantation.

## **Acknowledgments**

The authors are grateful to Dr. C. Fraker and Dr. K. G. Asfura for critical discussion on alginate encapsulation and in vitro assessments, to the personnel of the DRI Preclinical Cell Processing and Translational Models Core for their help with islet isolation, transplantation and management of diabetic mice, to the DRI Imaging Core for providing expertise on confocal imaging, and to the DRI Histology core headed by Kevin Johnson for their help with histological processing of all samples.

ACCEPTED

## References

1. Barton FB, Rickels MR, Alejandro R, et al. Improvement in outcomes of clinical islet transplantation: 1999-2010. *Diabetes Care*. 2012;35(7):1436-1445.
2. Basta G, Calafiore R. Immunoisolation of pancreatic islet grafts with no recipient's immunosuppression: actual and future perspectives. *Current Diabetes reports*. 2011;11(5):384-391.
3. O'Sullivan ES, Vegas A, Anderson DG, Weir GC. Islets transplanted in immunoisolation devices: a review of the progress and the challenges that remain. *Endocrine Reviews*. 2011;32(6):827-844.
4. Tuch BE, Keogh GW, Williams LJ, et al. Safety and viability of microencapsulated human islets transplanted into diabetic humans. *Diabetes Care*. 2009;32(10):1887-1889.
5. Faleo G, Lee K, Nguyen V, Tang Q. Assessment of Immune Isolation of Allogeneic Mouse Pancreatic Progenitor Cells by a Macroencapsulation Device. *Transplantation*. 2016;100(6):1211-1218.
6. Yang HK, Ham DS, Park HS, et al. Long-term Efficacy and Biocompatibility of Encapsulated Islet Transplantation With Chitosan-Coated Alginate Capsules in Mice and Canine Models of Diabetes. *Transplantation*. 2016;100(2):334-343.
7. Sasikala M, Rao GV, Vijayalakshmi V, et al. Long-term functions of encapsulated islets grafted in nonhuman primates without immunosuppression. *Transplantation*. 2013;96(7):624-632.
8. Zimmermann U, Mimietz S, Zimmermann H, et al. Hydrogel-based non-autologous cell and tissue therapy. *BioTechniques*. 2000;29(3):564-572, 574, 576 passim.

9. Draget KI, Skjak-Braek G, Smidsrod O. Alginate based new materials. *Int J Biol Macromol.* 1997;21(1-2):47-55.
10. Soon-Shiong P, Desai NP, Sanford PA, Heitz R, Sojomihardjo S. Crosslinkable polysaccharides, polycations and lipids useful for encapsulation and drug release. *Patent PCT/US92/09364. World International Property Organization.* 1993:1-52.
11. Mazaheri R, Atkison P, Stiller C, Dupre J, Vose J, O'Shea G. Transplantation of encapsulated allogeneic islets into diabetic BB/W rats. Effects of immunosuppression. *Transplantation.* 1991;51(4):750-754.
12. Duvivier-Kali VF, Omer A, Parent RJ, O'Neil JJ, Weir GC. Complete protection of islets against allojection and autoimmunity by a simple barium-alginate membrane. *Diabetes.* 2001;50(8):1698-1705.
13. Omer A, Duvivier-Kali V, Fernandes J, Tchipashvili V, Colton CK, Weir GC. Long-term normoglycemia in rats receiving transplants with encapsulated islets. *Transplantation.* 2005;79(1):52-58.
14. Wang T, Adcock J, Kuhlreiber W, et al. Successful allotransplantation of encapsulated islets in pancreatectomized canines for diabetic management without the use of immunosuppression. *Transplantation.* 2008;85(3):331-337.
15. Soon-Shiong P FE, Nelson R, Heintz R, Merideth N, Sandford P, Zheng T, Komtebedde J. Long-term reversal of diabetes in the large animal model by encapsulated islet transplantation. *Transplant Proc.* 1992;24(6):2946-2947.
16. Lanza RP, Jackson R, Sullivan A, et al. Xenotransplantation of cells using biodegradable microcapsules. *Transplantation.* 1999;67(8):1105-1111.

17. Lum ZP, Krestow M, Tai IT, Vacek I, Sun AM. Xenografts of rat islets into diabetic mice. An evaluation of new smaller capsules. *Transplantation*. 1992;53(6):1180-1183.
18. Sun Y, Ma X, Zhou D, Vacek I, Sun AM. Normalization of diabetes in spontaneously diabetic cynomolgus monkeys by xenografts of microencapsulated porcine islets without immunosuppression. *J Clin Invest*. 1996;98(6):1417-1422.
19. Paredes Juarez GA, Spasojevic M, Faas MM, de Vos P. Immunological and technical considerations in application of alginate-based microencapsulation systems. *Front Bioeng Biotechnol*. 2014;2:26.
20. Buchwald P. A local glucose-and oxygen concentration-based insulin secretion model for pancreatic islets. *Theor Biol Med Model*. 2011;8:20.
21. Omer A, Duvivier-Kali VF, Aschenbach W, Tchipashvili V, Goodyear LJ, Weir GC. Exercise induces hypoglycemia in rats with islet transplantation. *Diabetes*. 2004;53(2):360-365.
22. De Vos P, Vegter D, De Haan BJ, Strubbe JH, Bruggink JE, Van Schilfgaarde R. Kinetics of intraperitoneally infused insulin in rats. Functional implications for the bioartificial pancreas. *Diabetes*. 1996;45(8):1102-1107.
23. Colton CK, Avgoustiniatos ES. Bioengineering in development of the hybrid artificial pancreas. *J Bionic Eng*. 1991;113(2):152-170.
24. Calafiore R. Perspectives in pancreatic and islet cell transplantation for the therapy of IDDM. *Diabetes care*. 1997;20(5):889-896.
25. Elliott RB, Escobar L, Tan PL, et al. Intraperitoneal alginate-encapsulated neonatal porcine islets in a placebo-controlled study with 16 diabetic cynomolgus primates. *Transplant Proc*. 2005;37(8):3505-3508.



26. Bhujbal SV, Paredes-Juarez GA, Niclou SP, de Vos P. Factors influencing the mechanical stability of alginate beads applicable for immunoisolation of mammalian cells. *J Mech Behav Biomed Mater.* 2014;37:196-208.
27. Pileggi A, Molano RD, Berney T, et al. Prolonged allogeneic islet graft survival by protoporphyrins. *Cell Transplant.* 2005;14(2-3):85-96.
28. Berman DM, O'Neil JJ, Coffey LC, et al. Long-term survival of nonhuman primate islets implanted in an omental pouch on a biodegradable scaffold. *Am J Transplant.* 2009;9(1):91-104.
29. Morch YA, Donati I, Strand BL, Skjak-Braek G. Effect of Ca<sup>2+</sup>, Ba<sup>2+</sup>, and Sr<sup>2+</sup> on alginate microbeads. *Biomacromolecules.* 2006;7(5):1471-1480.
30. Tomei AA, Manzoli V, Fraker CA, et al. Device design and materials optimization of conformal coating for islets of Langerhans. *Proc Natl Acad Sci U S A.* 2014;111(29):10514-10519.
31. Cechin S, Alvarez-Cubela S, Giraldo JA, et al. Influence of in vitro and in vivo oxygen modulation on beta cell differentiation from human embryonic stem cells. *Stem Cells Transl Med.* 2014;3(3):277-289.
32. Najjar M, Manzoli V, Villa C, et al. Fibrin Gels Engineered with Pro-Angiogenic Growth Factors Promote Engraftment of Pancreatic Islets in Extrahepatic Sites in Mice. *Biotechnol Bioeng.* 2015.
33. Veisheh O, Doloff JC, Ma M, et al. Size- and shape-dependent foreign body immune response to materials implanted in rodents and non-human primates. *Nat Mater.* 2015;14(6):643-651.

## Figure Legends

**Figure 1. Optimizing fabrication of ALG Micro capsules to minimize the volume of encapsulated islet grafts.** (A) Schematic of our approach to determine the effects of capsule composition and transplant site on encapsulated graft outcomes. (B) Diameter distribution (n=300) of cell-free 1.2% UP-MVG microcapsules (ALG) fabricated with the optimized parameters (**Table 1**, bold). (C-D) Phase contrast images (C) and confocal images of live (green) /dead (red) stained (D) ALG microcapsules fabricated with optimized fabrication parameters (**Table 1**, bold) and loading density of pancreatic islets from Lewis Rats equal to 5k, 15k, and 30k IEQ/ml and compared to Naked islets; scale bars 100 $\mu$ m; nuclei: blue. (E-F) Glucose-stimulated insulin release (GSIR) of islets encapsulated in optimized fabrication parameters (**Table 1**, bold). Micro capsules loaded with 15k IEQ/ml rat islets (green) are compared to naked islets (black). N=3 aliquots of 100 IEQ per conditions from a minimum of n=3 independent experiments. Absolute values of insulin concentration in supernatants after incubation in low glucose (L1), high glucose (HG) and low glucose (L2) (E), and stimulation indexes (F) are indicated. (G) Diameter distribution (n=253 capsules from n=7 independent experiments) of islet-containing 1.2% UP-MVG microcapsules (ALG) fabricated with the optimized parameters (**Table 1**, bold).

**Figure 2. Effects of transplantation site on the outcome of islet allografts encapsulated in optimized ALG microcapsules (Micro) without immunosuppression. The free-floating intraperitoneal (IP) site is compared to the confined and vascularized epididymal fat pad (EFP) site.** (A) Blood glucose of STZ-induced diabetic C57BL/6 mice transplanted with 750 IEQ naked in the EFP (black, n=15) or IP (grey, n=8) sites or 750 IEQ microencapsulated

(Micro) in the EFP (green, n=7) or IP (orange, n=5) sites; all islets from fully MHC-mismatched BALB/c mice donors. **(B)** Percentage of mice that reversed diabetes after transplantation. **(C)** Percentage survival of allografts that reversed diabetes after transplantation. **(D-F)** Histological evaluation of EFP grafts and of capsules retrieved from the IP site by intraperitoneal lavage, fixed in formalin, embedded in paraffin, and thin sliced (5 $\mu$ m). Shown are grafts that reversed diabetes and maintained euglycemia for more than 100 days. In H&E stained sections **(D)** arrows point at areas of islet central necrosis. Scale bars 100 $\mu$ m. Confocal images: host vessels (CD31<sup>+</sup>, red), macrophages (MAC2<sup>+</sup>, green) and beta cells (INS<sup>+</sup>, cyan) are shown in panel **E**; T cells (CD3<sup>+</sup>, red), B cells (B220<sup>+</sup>, green) and beta cells (INS<sup>+</sup>, cyan) are shown in panel **F**. Nuclei are counterstained with DAPI (grey). Scale bar 150 $\mu$ m; **(G)** Phase contrast images of baboon islets encapsulated in Micro capsules fabricated with optimized fabrication parameters (**Table 1**, bold) and loading density of 15k IEQ/ml and compared to Naked islets. Scale bars 200 $\mu$ m; **(H)** Blood glucose of STZ-induced diabetic NOD-scid mice transplanted with 1000 IEQ naked (black, n=5) or 750 IEQ microencapsulated (Micro, green, n=4) islets in the EFP and compared to 1000 IEQ (light grey) and to 2000 IEQ (dark grey) naked islets transplanted in the kidney capsule (KD) controls; all islets from baboon non-human primate donors. **(I)** Percentage of mice that reversed diabetes after transplantation of baboon islets. **(J)** Histological evaluation of EFP grafts of naked vs. Micro encapsulated in the EFP site analyzed 30 days after transplantation in diabetic NOD-scid mice. Scale bars 200 $\mu$ m.

**Figure 3. Design, fabrication and in vitro evaluation of PEG-ALG hybrid MicroMix and Double capsules compared to ALG Micro capsules.** **(A-B)** Osmotic pressure resistance of cell-free ALG capsules (Micro) compared to PEG capsules and ALG-PEG capsules (MicroMix).

Percentage of intact Micro (n=30) vs. PEG (n=30) vs. ALG-PEG (n=30) capsules after exposure to 2hrs ddH<sub>2</sub>O followed by saline buffer for 60 minutes (**A**) and % intact capsule dependence on time exposure to saline (**B**). (**C**) Schematic of ALG **Micro** vs. hybrid ALG-PEG **Micromix** capsules, where PEG and ALG are interlaced, and **Double** capsules, where PEG is added to the ALG Micro capsule as a thin external layer. (**D**) Schematic of the emulsion procedure for fabrication of Double capsules. (**E**) Representative phase contrast (top) and confocal images (bottom) of Lewis rat islets enclosed in Micro, Micromix and Double capsules stained with anti-PEG antibodies (green). Nuclei are counterstained with Hoechst (blue). Thickness of double capsules was quantified on n=12 capsules and was found to be 15±2 μm. Scale bars 100 μm. (**F-H**) Diameter distribution of islet-containing MicroMix (blue, **F**) and Double (purple, **G**) capsules and direct comparison with Micro capsules (**H**, p>0.05). In panel H, statistical analysis of the measured values is presented in the table next to the graph. (**I**) Viability assessment by live (green) and dead (red) staining via confocal imaging of Lewis rat islets enclosed in Micro, Micromix, and Double capsules 48 hours after encapsulation. Nuclei are counterstained with Hoechst (blue). Scale bar 100 μm. (**J**) Glucose-stimulated insulin release (GSIR) of Lewis rat islets encapsulated in Micro (green), MicroMix (blue), Double (purple) capsules and compared to naked islets (black). Absolute insulin secretion and stimulation index are indicated. N=3 aliquots of 100 IEQ per conditions from a minimum of n=3 independent experiments. (**K**) Oxygen consumption rate (OCR) normalized to total DNA content of Lewis rat islets encapsulated in Micro (green), MicroMix (blue), Double (purple) capsules and compared to naked islets (black); n=3 per condition.

**Figure 4. Effects of composition of PEG-ALG capsules on the outcome of islet allografts in the IP site without immunosuppression.** ALG Micro capsules are compared to PEG-ALG hybrid MicroMix and Double capsules containing islets and to naked islets. **(A)** Blood glucose of STZ-induced diabetic C57BL/6 mice transplanted with 750 IEQ naked (grey, n=7) or encapsulated in Micro (orange, n=4), or MicroMix (blue, n=4), or Double (purple, n=6) capsules in the IP; all islets from fully MHC-mismatched BALB/c mice donors. **(B)** Percentage of mice that reversed diabetes after transplantation. **(C)** Percentage survival of allografts that reversed diabetes after transplantation. **(D-F)** Histological evaluation of grafts retrieved from the IP site by intraperitoneal lavage, fixed in formalin, embedded in paraffin, and thin sliced (5 $\mu$ m). Shown are grafts that reversed diabetes and maintained euglycemia for more than 100 days. In H&E stained sections **(D)** arrows point at areas of islet necrosis. Scale bars 100 $\mu$ m. Confocal images: host vessels (CD31<sup>+</sup>, red), macrophages (MAC2<sup>+</sup>, green) and beta cells (INS<sup>+</sup>, cyan) are shown in panel **E**; T cells (CD3<sup>+</sup>, red), B cells (B220<sup>+</sup>, green) and beta cells (INS<sup>+</sup>, cyan) are shown in panel **F**. Nuclei are counterstained with DAPI (grey). Scale bar 150 $\mu$ m.

**Figure 5. Effects of composition of PEG-ALG capsules on the outcome of islet allografts in the EFP site without immunosuppression.** ALG Micro capsules are compared to PEG-ALG hybrid MicroMix and Double capsules and to naked islets. **(A)** Blood glucose of STZ-induced diabetic C57BL/6 mice transplanted with 750 IEQ naked (black, n=15) or encapsulated in Micro (green, n=7), or MicroMix (blue, n=4), or Double (purple, n=6) capsules in the EFP; all islets from fully MHC-mismatched BALB/c mice donors. **(B)** Percentage of mice that reversed diabetes after transplantation. **(C)** Percentage survival of allografts that reversed diabetes after transplantation. **(D-F)** Histological evaluation of EFP grafts fixed in formalin, embedded in

paraffin, and thin sliced (5 $\mu$ m). Shown are grafts that reversed diabetes and maintained euglycemia for more than 100 days. In H&E stained sections (**D**) arrows point at area of host reactivity. Scale bars 100 $\mu$ m. Confocal images: host vessels (CD31<sup>+</sup>, red), macrophages (MAC2<sup>+</sup>, green) and beta cells (INS<sup>+</sup>, cyan) are shown in panel **E**; T cells (CD3<sup>+</sup>, red), B cells (B220<sup>+</sup>, green) and beta cells (INS<sup>+</sup>, cyan) are shown in panel **F**. Nuclei are counterstained with DAPI (grey). Scale bar 150 $\mu$ m. (**G-I**) Biocompatibility of cell-free Micro (**G**), MicroMix (**H**) and Double (**I**) capsules in the EFP site: H&E staining (top) and Masson's Trichrome (bottom), 7 days after implantation. Scale bar 100 $\mu$ m.

### **Table Legends**

#### **Table 1**

Average diameter and standard deviation (SD) of cell-free ALG microcapsules (Micro) as a function of the Needle internal (ID) and external (OD) diameter (top) and the ALG extrusion flow rate (bottom) in the electrostatic droplet generator process. The parameters that we varied are highlighted in grey and the parameters that we chose for studies with islets are highlighted in bold.

Figure 1

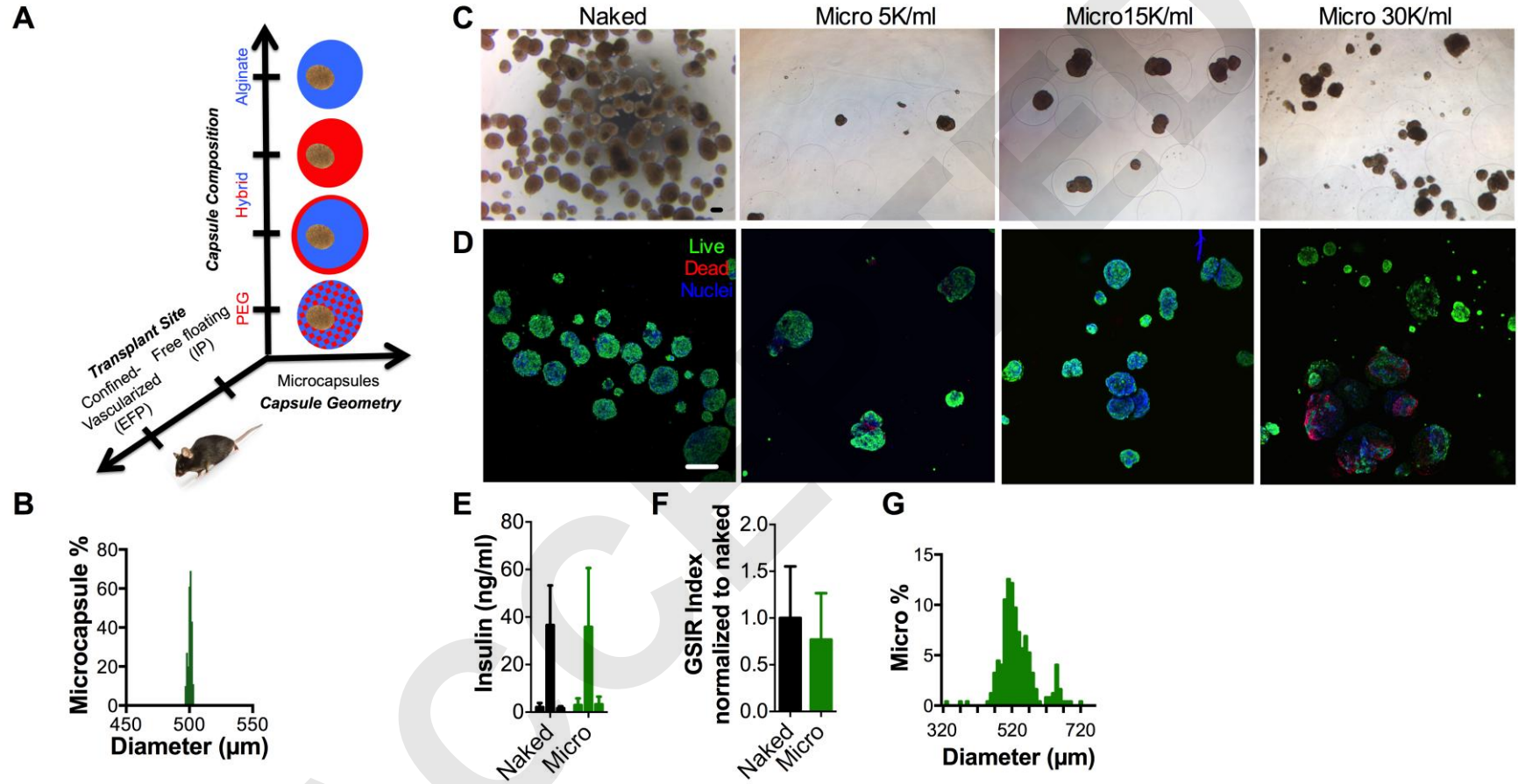


Figure 2

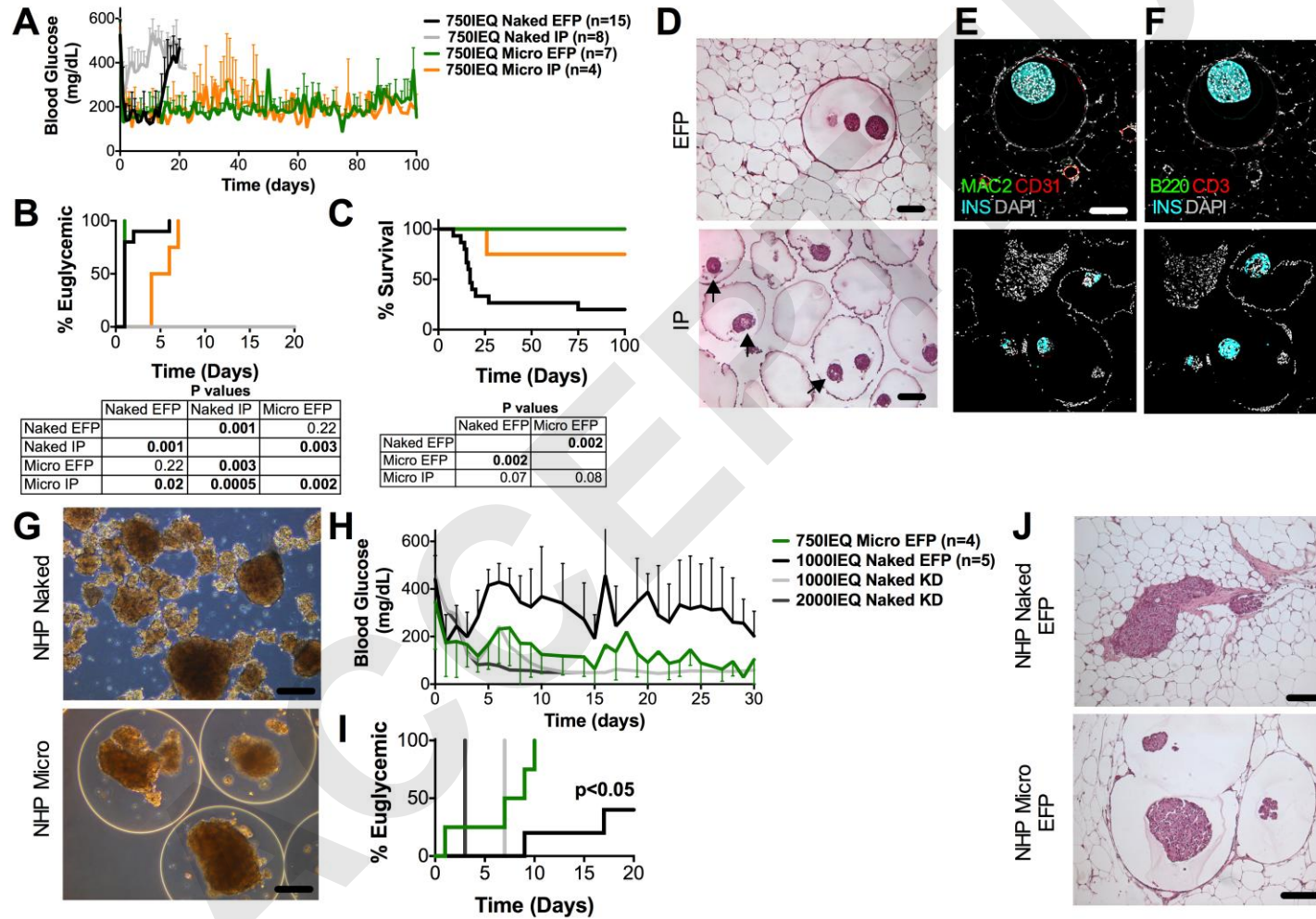




Figure 3

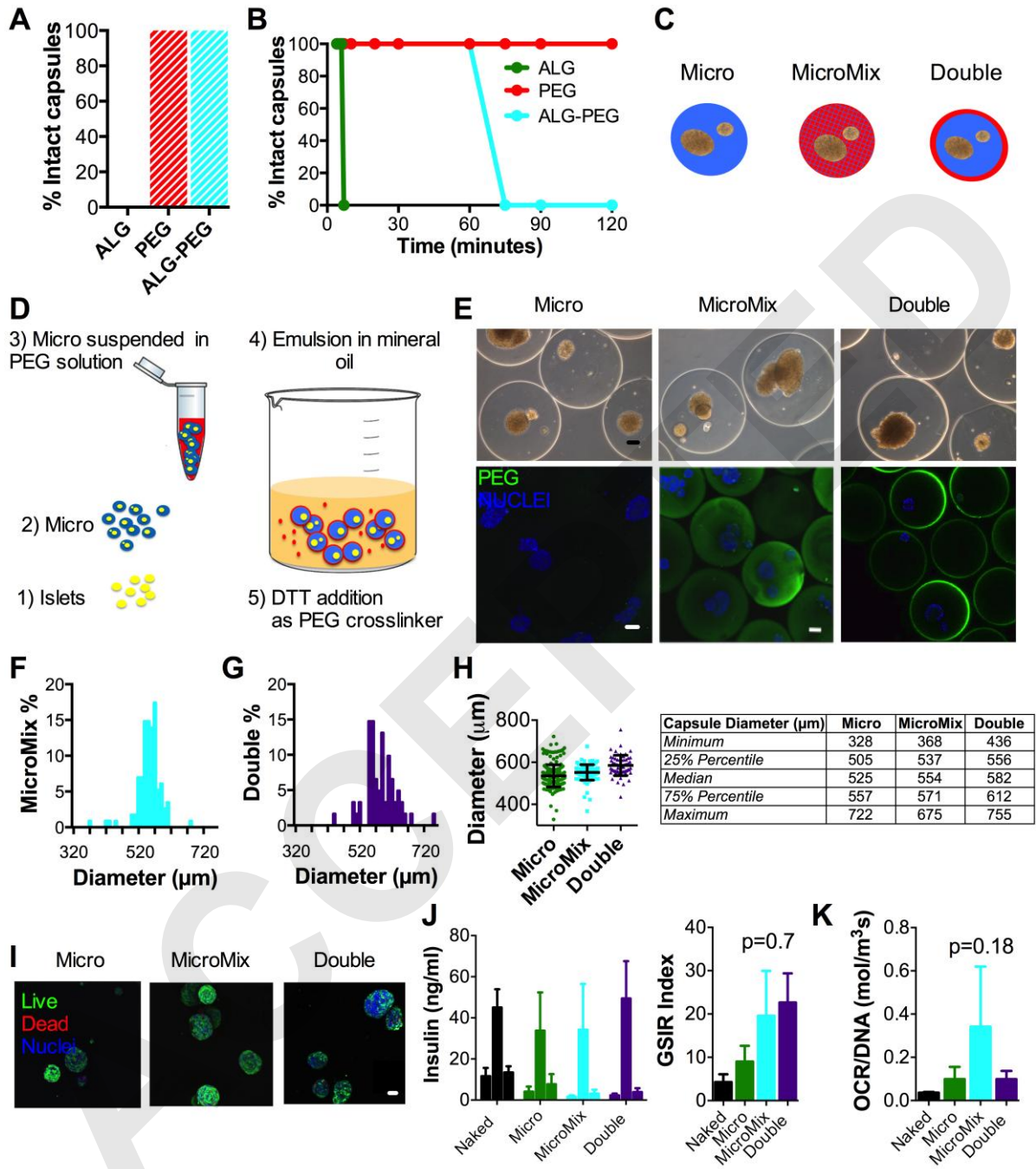


Figure 4

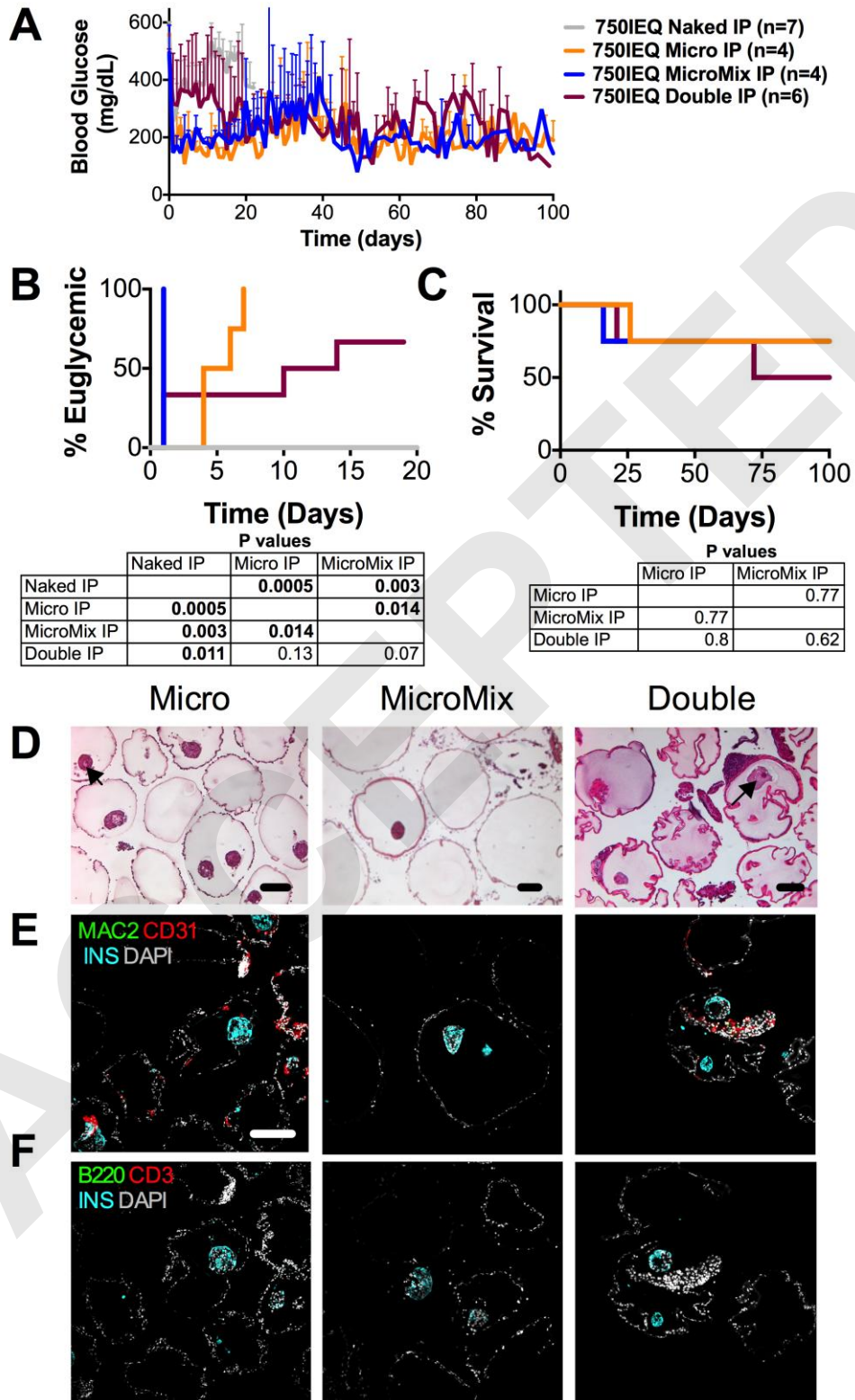


Figure 5

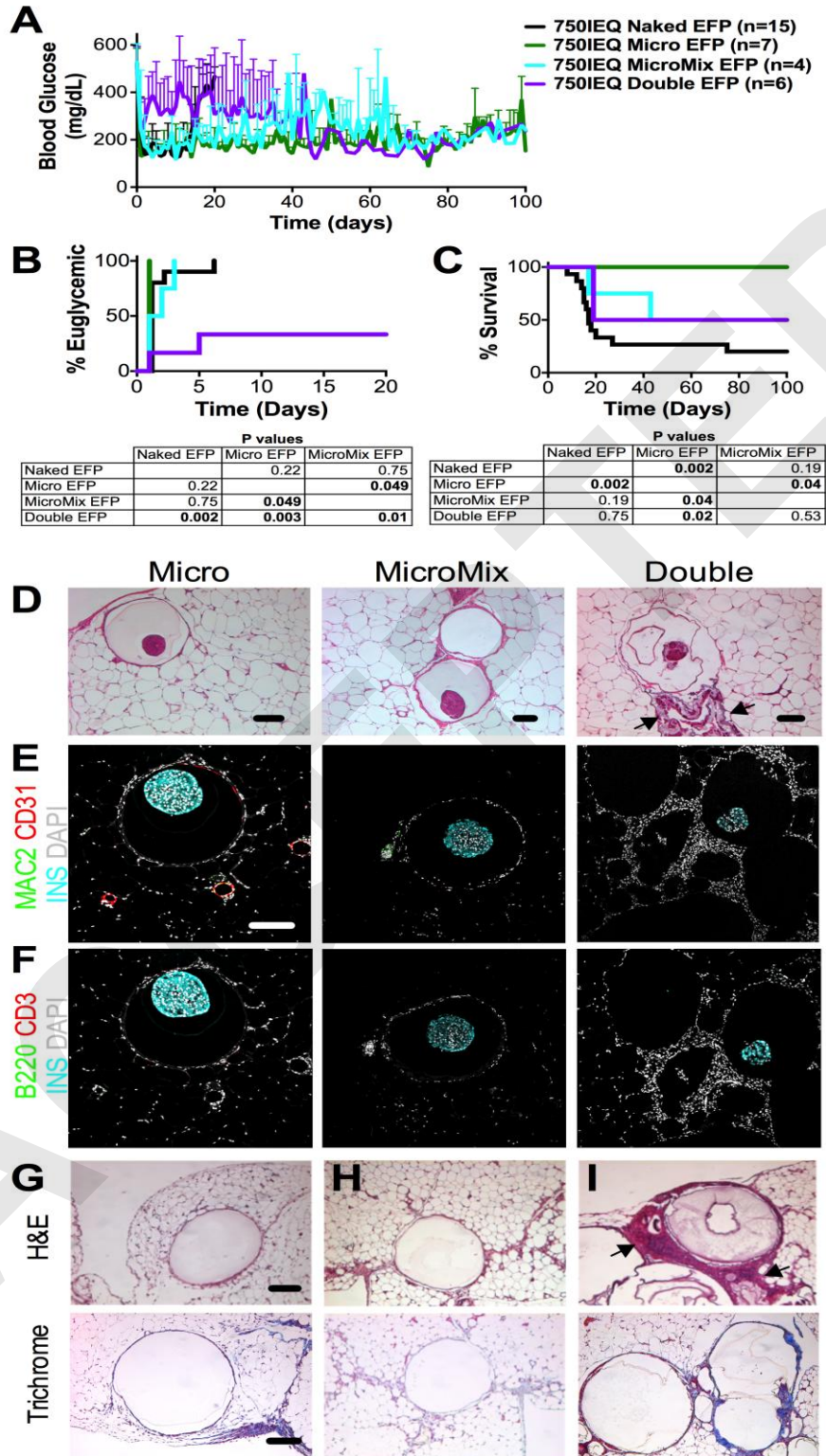


Table 1

Needle Diameter (mm)		Micro Diameter ( $\mu\text{m}$ )	
OD	ID	Average	SD
0.7	0.17	279	29
<b>0.7</b>	<b>0.4</b>	<b>500</b>	<b>17</b>
0.9	0.6	749	35

Alginate Flow Rate ( $\mu\text{l}/\text{min}$ )	Micro Diameter ( $\mu\text{m}$ )	
	Average	SD
5	526	48
<b>10</b>	<b>502</b>	<b>8</b>
25	621	16
50	651	12

## Supplemental Materials & methods

### Materials and methods

#### **Encapsulation materials.**

For Micro capsule fabrication, ultra-pure medium viscosity (>200 mPa\*s) sodium alginate composed of 60% guluronate units (UP-MVG alginate, Novamatrix) was dissolved overnight in Hank's Balanced Salt Solution buffer without calcium and magnesium ions (HBSS w/o Ca<sup>2+</sup> Mg<sup>2+</sup>, Gibco) to a working concentration of 1.2% w/v. 50mM calcium chloride (CaCl<sub>2</sub>) gelation solution was prepared by dissolving 5.55mg CaCl<sub>2</sub>, 2.09mg 3-(N-Morpholino) propanesulfonic acid 4-Morpholinepropanesulfonic acid (MOPS), 25.5mg D-mannitol and 0.25mL Tween (Sigma-Aldrich) in 1L Milli-Q H<sub>2</sub>O. The final osmolarity of the gelation solution was 300 mOsm, iso-osmotic with cells.

For MicroMix capsule fabrication of 1.2% UP-MVG - 5% PEG-MAL final composition, a solution of 5% (w/v) polyethylene glycol (PEG), functionalized (75%) with maleimide groups (PEG-MAL, 10kDa, 8-arms, Jenkem Technology custom synthesis) was obtained by dissolving 50mg of PEG-MAL in 1ml of 1.2% UP-MVG solution.

For Double capsule fabrication, PEG-MAL was dissolved in HBSS w/o Ca<sup>2+</sup> Mg<sup>2+</sup> at 5% w/v concentration. The crosslinking solution for the PEG component of MicroMix capsules was prepared by dissolving 2.31mg of Dithiothreitol (DTT, OmniPur, Calbiochem) in 1ml HBSS w/ Ca<sup>2+</sup>, Mg<sup>2+</sup>, in order to obtain a 3:1 molar ratio of DTT (two reactive groups) to PEG (8-arm 75% functionalization - six reactive groups). The DTT cross-linking solution for the Double capsules was prepared by dissolving 102mg DTT in 333μl Dimethyl sulfoxide (DMSO, Sigma), which gives a final concentration of DTT in the 50ml emulsion of 2mg/ml in order to obtain a 3:1 molar ratio of DTT to PEG.

## **Islet isolation**

Male BALB/c mice (Jackson Laboratories) and Lewis rats (Envigo Laboratories, formerly Harlan) were housed in virus antibody free (VAF) rooms in micro isolated cages and exposed to a 12-h light/dark cycle with ad libitum access to autoclaved food and water. Mice were used as islet donors at 10-12 weeks of age. Rats were used as islet donors at 250-280g weight. Animal studies were performed under protocols reviewed and approved by the University of Miami Institutional Animal Care and Use Committee (protocol 13-042). Islets were isolated by liberase (Roche) digestion followed by purification on Euroficoll density gradients (Mediatech), as described elsewhere <sup>1</sup>. Protocols were optimized with rat islets because of the higher isolation yield per animal.

Non-human primate baboon (NHP; The Mannheimer Foundation, Inc., Homestead, FL, USA) islets were isolated using previously described methods <sup>2</sup>.

All islets were cultured in CMRL 1066 (Mediatech) supplemented with 10% FBS (Gibco), 1% penicillin–streptomycin (Gibco), 2.5% 1M HEPES and 1% L-glutamine (Gibco).

## **Optimization of encapsulation parameters for fabrication of cell-free and islet-loaded Micro and MicroMix capsules.**

An electrostatic droplet generator (Nisco) was utilized to fabricate alginate Micro and MicroMix capsules. Voltage differences between needle and gelling solution in the collection vessel, alginate solution flow rate, and cell-loading density were varied to minimize capsule size. 1.2% UP-MVG (Micro) or 1.2% UP-MVG - 5% PEG-MAL (MicroMix) hydrogel precursor solutions were extruded through a blunt stainless steel needle using a syringe pump (Harvard Apparatus, Holliston, MA) and a 3mL plastic syringe (BD). Three needles with internal diameters equal to

0.17, 0.4, and 0.6 mm and external diameters of 0.7, 0.7, and 0.9 mm respectively were evaluated. A potential difference between 8.8 and 10kV was applied between the needle and the CaCl<sub>2</sub> gelling solution. A distance of 2 to 4cm between the needle and the gelling solution was tested; the flow rate of hydrogel precursor solutions was varied between 5 to 50µl/min. After extrusion, Micro and MicroMix capsules were allowed to cross-link in the CaCl<sub>2</sub> bath for 10 minutes<sup>3</sup>. Next, the ionically gelled microcapsules were washed 3 times in HBSS w/ Ca<sup>2+</sup>, Mg<sup>2+</sup>, whereas MicroMix capsules were washed only once in HBSS w/ Ca<sup>2+</sup>, Mg<sup>2+</sup>, followed by the addition of 1ml of DTT solution for 1 minute to cross-link the PEG-MAL network. MicroMix capsules were then washed three times in HBSS w/ Ca<sup>2+</sup>, Mg<sup>2+</sup>. A sample of 30 microcapsules from each cell-free run was taken (n=3) and the capsules were imaged using a light microscope (LEICA DMIL, Germany). Images were processed with Image J (National Institute of Health) to determine capsule diameter. For encapsulation, isolated pancreatic islets were suspended in 100µl of 1.2% UP-MVG alginate (Micro) or in 1.2% UP-MVG - 5% PEG-Mal (MicroMix) hydrogel precursor solutions. Three islet loading densities were evaluated: 5,000, 15,000 and 30,000 IEQ/ml. The islet suspensions in the hydrogel precursor solutions were extruded through a 0.4mm diameter needle at 10 µl/min by a syringe pump and a voltage difference between the needle and the gelling solution of 8.8kV was applied. The diameter of islet-containing microcapsules was measured on a sample of n=15-60 capsules for each encapsulation batch to guarantee reproducibility of the encapsulation process.

### **Fabrication of PEG Micro capsules**

5% PEG (75% functionalized PEG-maleimide 10kDa 8arms, Jenkem) capsules were obtained by adapting a previously reported method<sup>4</sup>. The method consists of hand-pipetting PEG (pre-mixed

with DTT at pH 4-5) into polypropylene glycol (PPG, Sigma) containing 0.02% triethanolamine (Sigma) and 10% Span-80 (Sigma) followed by purification by hexane extraction of the oil phase<sup>4</sup>. The process is designed to promote PEG crosslinking and mold the capsules into spheres of comparable size and geometry to alginate Micro capsules.

### **Osmotic pressure test**

Evaluation of mechanical stability of microcapsules was performed by osmotic pressure testing as previously described<sup>5</sup>. ALG Micro and PEG-ALG MicroMix capsules were resuspended in Hank's balanced salt solution (HBSS, 270-305 mOsm/kg). Thirty capsules for each formulation were hand-picked and transferred to 10 wells of a 24-well-plate (3 beads/well). Capsule diameter was imaged with a Leica light microscope and measured with Leica Application Suite. Then, the HBSS supernatant was removed and the capsules were incubated for 2 hours at 37°C in 1ml/well of ddH<sub>2</sub>O (0 mOsm/kg). At the end of this incubation period, capsules were imaged, the supernatant was removed and replaced with 1 ml/well saline-10mM HEPES (308 mOsm/kg) supplemented with 1 drop/well of trypan blue. Percentage of fractured or swollen capsules was quantified over the following 2 hours.

### **Fabrication of Double capsules: double coating of Micro capsules with PEG by emulsion technology.**

To fabricate Double capsules, 100µl of UP-MVG Micro capsules were suspended in 1ml of 5% PEG-MAL (water phase). A solution of 50ml light mineral oil (Sigma Aldrich) and 5% Span80 (Sigma Aldrich) (oil phase) was formed by stirring at 350rpm for 2'. The water phase was added



drop-by-drop to the center of the oil phase while the oil phase was continuously stirred at 350rpm. Five minutes after addition of the water phase to the oil phase, the DTT solution in DMSO was added to induce PEG-MAL gelation and the stirring speed was increased to 450rpm. PEG double coating was allowed to crosslink for 15 minutes while stirring as previously reported<sup>4</sup>. Then Double capsules were extensively washed with HBSS w/  $\text{Ca}^{2+}$ ,  $\text{Mg}^{2+}$  and secondary beads were removed by filtration through a 250 $\mu\text{m}$  cell strainer (Thermo Scientific).

In order to increase the efficiency of purification of Double capsules from secondary cell-free PEG-MAL beads, the fabrication protocol was further optimized. First, the initial stirring speed was increased from 350 rpm to 400 rpm. Then, the water phase was added to the oil phase and stirred at 400 rpm. Four minutes later, the stirring speed was further increased to 500 rpm for one minute before adding the DTT solution. Finally, the capsules were extensively washed with HBSS w/  $\text{Ca}^{2+}$ ,  $\text{Mg}^{2+}$ .

#### ***In vitro* assessment of viability and functionality of encapsulated islets.**

Static glucose-stimulated insulin release (GSIR) was utilized for assessment of islet function. GSIR was performed to compare *in vitro* function of encapsulated islets to uncoated islets (naked control) as previously described<sup>4</sup>. Briefly, islet aliquots per conditions (100 IEQ; n=3) were loaded within a Sephadex (G-10; GE Healthcare) slurry into microchromatography columns (BioRad) and incubated in low-glucose (LG) Krebs buffer (2.2mM or 40mg/dL D-glucose, Sigma) for 1 h at 37°C for equilibration and pre-incubation. This was followed by sequential incubations for 1 h each in low glucose (LG, 2.2mM or 40mg/dL), high glucose (HG, 16.7mM or 300mg/dL), and again LG buffer. At the end of each incubation period, 1mL of eluate was collected by adding 1mL of LG solution to each column. Insulin concentrations (ng/ml) in eluted

samples were assessed by rat or mouse ELISA (Mercodia). GSIR results were presented as absolute values of insulin concentration in eluates from stimulation with LG1, HG, and LG2, and as stimulation indexes (GSIR Index, calculated as the ratio of insulin released after exposure to HG to insulin released after exposure to LG1). Indexes shown are the average of a minimum of n=3 independent experiments and have been normalized to their naked control indexes.

For viability assessment, naked and encapsulated islets were stained with calcein-AM (live cell marker) and ethidium bromide (dead cell marker) (live/dead viability kit, Molecular Probes), and imaged with a Leica SP5 inverted confocal microscope. Z-scans of up to 200µm volumes were performed (Slice thickness, 5µm).

Oxygen Consumption Rate (OCR) measurements were performed as previously described <sup>6</sup>. Briefly, aliquots of approximately 500 IEQ (n=3) were used for measurements of OCR in temperature controlled, sealed and stirred microchambers (Instech Co., Plymouth Meeting, PA, <http://www.instechlabs.com>). Oxygen consumption rate per unit time was quantified as in the following equation:  $OCR = \Delta[O_2]/\Delta t * V$ , where OCR is the cellular oxygen consumption rate in mol/m<sup>3</sup>\*s and  $\Delta t$  is the change in time in seconds,  $\Delta[O_2]$  is the change in oxygen concentration in moles, and V is the chamber volume in liters. After measurements were completed, cells were collected from the chambers, solubilized in the DNA extraction buffer provided by the manufacturer, and DNA was extracted following manufacturer's protocol using the DNAeasy Blood and Tissue Kit (Qiagen). DNA was quantified using the Quant-iT PicoGreen assay (Invitrogen). Cell number was estimated using a previously reported value of 6 pg of DNA per single cell. Total tissue volume was then derived using the calculated cell number and single cell volume using the following equation:  $V = 4/3 N \pi R^3$  where V is the total tissue volume, N is the

cell number, and R is the average radius of the cells,  $5 * 10^{-6}$  m. Data are presented as OCR normalized to total DNA content.

### **Engineered fibrin gels**

Fibrin gels were engineered for promoting rapid revascularization of embedded islets as previously described <sup>7</sup> generating pro-angiogenic resorbable scaffolds for naked and encapsulated islets. For this study, pro-angiogenic resorbable scaffolds comprised

- 2 $\mu$ M (102 $\mu$ g/ml) of fibronectin (FN) fragment, containing an integrin-binding domain (FN 9-10), a growth factor (GF)-binding domain (FN 12-14) and a fibrin binding substrate for factor XIIIa, synthesized as previously described <sup>8</sup>, kindly provided by Dr. Jeffrey Hubbell
- 8mg/ml human fibrinogen depleted of fibronectin, plasminogen, and von Willebrand factor (Enzyme Research Laboratories, South Bend, IN, USA)
- 17 $\mu$ g/ml aprotinin (Sigma-Aldrich)
- 2U/ml human thrombin (Sigma-Aldrich)
- 8U/ml factor XIIIa (Fibrogammin; Behring, Marburg, Germany)
- 2.5mM CaCl<sub>2</sub> in HEPES buffer (Sigma)
- 101nM (25ng/gel) human platelet-derived growth factor-BB (PDGF-BB, carrier-free from R&D Systems)
- 130nM (50ng/gel) human vascular endothelial growth factor-A165 (VEGF-A165, carrier-free from R&D Systems)

### **Diabetes Induction and Islet Transplantation in Mice.**

Diabetes was induced in islet recipients, C57BL/6 mice, by a single i.v. injection of streptozotocin (200 mg/kg; Sigma–Aldrich). Mice were considered diabetic after three consecutive readings of blood glucose  $>350\text{mg/dL}$ . For transplantation of either naked islets or microcapsules in the epididymal fat pad (EFP), a small cutaneous incision, followed by a small muscular incision, were performed on the abdomen of recipient mice under general anesthesia (isoflurane). The EFP was then gently exposed and flattened. 750 IEQ naked islets were collected from the culture dish with a Hamilton syringe, pelleted by gravity, and distributed uniformly on the surface of the EFP while microcapsules containing 750IEQ were distributed on the EFP with a spatula. To immobilize the islets to the EFP membrane and enhance graft revascularization, 20 $\mu\text{l}$  of engineered fibrin gels were then pipetted on the EFP to cover the islets. Fibrin gelation was allowed to occur *in situ*, resulting in cell immobilization within the pro-angiogenic fibrin scaffolds and in close contact to the host vascular supplies provided by the EFP membrane. An EFP pocket was created by wrapping the islets plus the scaffold-containing EFP. GF-free and FN fragment-free fibrin glue was used to seal the ‘EFP pocket’ and prevent unwrapping during long-term implantation. The EFP pocket containing the graft was gently placed back in the abdominal cavity of the mouse then proceeded to suture the muscle and the skin.

Graft function was monitored by measuring non-fasting blood glucose values using portable glucometers (OneTouch Ultra 2; LifeScan). Reversal of diabetes was considered when mice maintained at least three consecutive blood glucose readings  $< 250\text{mg/dL}$  after islet transplantation. Graft rejection was considered when at least three consecutive blood glucose readings  $> 250\text{mg/dL}$  were detected in those mice that reversed diabetes following islet

transplantation. To confirm graft function and exclude pancreas regeneration in mice that reversed diabetes after transplantation, EFP grafts were removed 100 days after transplantation and mice were monitored until return to hyperglycemia was reached.

For intraperitoneal (IP) islet transplantation, a small incision in the skin followed by an incision along the linea alba of the peritoneum were performed under general anesthesia (isoflurane). Naked islets and islets-containing microcapsules were suspended in HBSS w/  $\text{Ca}^{2+}$   $\text{Mg}^{2+}$ , collected with a 1ml micropipette, and injected into the peritoneal cavity in a total volume of approximately 0.2 ml. Muscle and skin were then sutured. After sacrificing the mice by cervical dislocation, capsules were retrieved by intraperitoneal lavage with HBSS w/  $\text{Ca}^{2+}$   $\text{Mg}^{2+}$ .

Transplantation in the renal subcapsular space (KD) was performed as previously described<sup>4</sup>. Briefly, a small incision in the back of the mouse was performed under general anesthesia (isoflurane) and the kidney was exposed. A microsurgical scissor was then used to make a small incision in the kidney capsule. The islets were collected using a Hamilton syringe and pelleted in a PE-50 tubing, which was then connected to the syringe and used to gently distribute the islets under the capsule. Kidney capsule was cauterized and muscle and skin sutured.

### **Graft histological evaluation**

Formalin-fixed grafts were embedded in paraffin, sectioned (5 $\mu\text{m}$ ), and processed for standard H&E histology or for immunofluorescence. Antigen retrieval (sodium citrate buffer) was performed before proceeding with immunofluorescence staining. For immunofluorescence staining, samples were permeabilized in 0.2% Triton X-100 (Sigma) at RT for 5-10 min, then blocked in 2% bovine serum albumin (Sigma) and 10% serum (Sigma) of the host of the secondary antibody in phosphate buffered saline (PBS, Invitrogen) for 90 min at RT. Primary

antibodies were prepared at working concentrations in 2% BSA in PBS and tissue sections were incubated overnight at 4°C. Secondary antibodies were purchased from Molecular Probes (Eugene, OR) and prepared at 1:200 working concentration in 2% BSA in PBS. Tissue sections were incubated for 1 hr at RT. 4',6 diamino-2-phenylindole (DAPI; Molecular Probes) was used for nuclear staining. Islets were identified by insulin<sup>+</sup> beta cells (guinea pig, 1:100; cat# A0564, Dako, Carpinteria, CA). Blood vessels were identified by CD31<sup>+</sup> (rabbit, 1:20, cat# AB28364, Abcam, Cambridge, MA). Macrophages were identified by Mac2 (rat, 1:500, cat# CL8942AP, Cedarlane, Burlington, NC), T cells by CD3 (rabbit, 1:500, cat# CMC10317022, Cell Marque, Rocklin, CA) and B cells by B220 (rat, 1:200, cat# 14-0452-82, eBioscience, San Diego, CA).

Images were acquired with a Leica DMIRB microscope for histological staining or with a Leica SP5 inverted confocal microscope for fluorescence imaging and processed with the Leica Application Suite software and ImageJ 3D (National Institutes of Health).

**Statistics.** Prism 5.0 (Graphpad, San Diego, CA) was used for statistical analysis. Unless otherwise noted, data are presented as mean  $\pm$  SD. Statistical comparisons were based on Student's t-test (two groups comparison) or analysis of variance (ANOVA) with Tukey post-hoc test for pairwise comparisons (for >2 groups comparisons). A confidence level of 95% was considered significant. Actuarial survival curves and log-rank test were used to compare diabetes reversal and graft survival amongst experimental groups. The statistical significance of differences between more than two groups for GSIR and cytotoxicity assay was analyzed by post-hoc Dunn's multiple comparison test.

## References:

1. Pileggi A, Molano RD, Berney T, et al. Prolonged allogeneic islet graft survival by protoporphyrins. *Cell transplantation*. 2005;14(2-3):85-96.
2. Berman DM, O'Neil JJ, Coffey LC, et al. Long-term survival of nonhuman primate islets implanted in an omental pouch on a biodegradable scaffold. *American journal of transplantation : official journal of the American Society of Transplantation and the American Society of Transplant Surgeons*. 2009;9(1):91-104.
3. Bhujbal SV, Paredes-Juarez GA, Niclou SP, de Vos P. Factors influencing the mechanical stability of alginate beads applicable for immunoisolation of mammalian cells. *Journal of the mechanical behavior of biomedical materials*. 2014;37:196-208.
4. Tomei AA, Manzoli V, Fraker CA, et al. Device design and materials optimization of conformal coating for islets of Langerhans. *Proc Natl Acad Sci U S A*. 2014;111(29):10514-10519.
5. Morch YA, Donati I, Strand BL, Skjak-Braek G. Effect of Ca<sup>2+</sup>, Ba<sup>2+</sup>, and Sr<sup>2+</sup> on alginate microbeads. *Biomacromolecules*. 2006;7(5):1471-1480.
6. Cechin S, Alvarez-Cubela S, Giraldo JA, et al. Influence of in vitro and in vivo oxygen modulation on beta cell differentiation from human embryonic stem cells. *Stem cells translational medicine*. 2014;3(3):277-289.
7. Najjar M, Manzoli V, Villa C, et al. Fibrin Gels Engineered with Pro-Angiogenic Growth Factors Promote Engraftment of Pancreatic Islets in Extrahepatic Sites in Mice. *Biotechnology and bioengineering*. 2015.

8. Martino MM, Tortelli F, Mochizuki M, et al. Engineering the growth factor microenvironment with fibronectin domains to promote wound and bone tissue healing. *Science translational medicine*. 2011;3(100):100ra189.

ACCEPTED